Journal of
Materials Chemistry B

Accepted Manuscript

This is an *Accepted Manuscript*, which has been through the RSC Publishing peer review process and has been accepted for publication.

Accepted Manuscripts are published online shortly after acceptance, which is prior to technical editing, formatting and proof reading. This free service from RSC Publishing allows authors to make their results available to the community, in citable form, before publication of the edited article. This *Accepted Manuscript* will be replaced by the edited and formatted *Advance Article* as soon as this is available.

To cite this manuscript please use its permanent Digital Object Identifier (DOI®), which is identical for all formats of publication.

More information about *Accepted Manuscripts* can be found in the **Information for Authors**.

Please note that technical editing may introduce minor changes to the text and/or graphics contained in the manuscript submitted by the author(s) which may alter content, and that the standard **Terms & Conditions** and the **ethical guidelines** that apply to the journal are still applicable. In no event shall the RSC be held responsible for any errors or omissions in these *Accepted Manuscript* manuscripts or any consequences arising from the use of any information contained in them.

Journal of Materials Chemistry B

Dynamic Article Links ►

Cite this: DOI: 10.1039/c0xx00000x

www.rsc.org/xxxxxx

COMMUNICATION

A metal-catalyst free flexible and free-standing chitosan/vacuum-stripped graphene/polypyrrole three dimensional electrode interface for high performance dopamine sensing†

Jing Liu, Ziming He, Jingwen Xue and Timothy Thatt Yang Tan*

Received (in XXX, XXX) Xth XXXXXXXXX 20XX, Accepted Xth XXXXXXXXX 20XX
DOI: 10.1039/b000000x

A three dimensional chitosan/vacuum-stripped graphene/ polypyrrole interface with hierarchical porous structure was fabricated as a free-standing and flexible electrochemical sensing electrode for dopamine detection, which exhibits unprecedented good selectivity, high sensitivity (632.1 μA mM^{-1} cm^{-2}), wide linear response range (0.1-200 μM), low detection limit (19.4 nM, *S/N* = 3) and good sensing performance in human serum samples, outperforming previously reported 2D and 3D graphene and/or PPy modified electrode, and exhibiting comparable performance with Au modified electrode.

Dopamine (DA), a crucial catecholamine neurotransmitter, plays important physiological roles in the central nervous, renal, hormonal and cardiovascular systems.[1, 2] The deficiency of DA neurotransmitter is associated with various serious disorders and diseases, such as senile dementia, Parkinson's disease, schizophrenia, epilepsy and HIV infection.[3, 4] Therefore, a key challenge is to develop simple, reliable and highly sensitive techniques for DA detection.

Electrochemical sensing of DA is simple, inexpensive and shows high sensitivity. However, the electrochemical detection of DA in biological samples is usually interfered by the coexisting ascorbic acid (AA) and uric acid (UA), which have similar oxidation potentials with DA.[5] The sensitivity and selectivity of electrochemical DA sensors have been improved by modifying a conventional solid electrode, such as glassy carbon electrode (GCE)[6-9] and gold electrode[10] with various nanostructured materials including conductive polymers, metal complex and carbon nanomaterials to increase the active surface area and enhance the specific interaction with DA. Due to the planar nature of the conventional solid electrodes, the performance enhancement of such sensors is limited.

Recently, a three-dimensional (3D) graphene foam fabricated by chemical vapor deposition was explored as DA detection sensor, and showed remarkable sensitivity due to high conductivity of the graphene and large specific surface area from well-defined macroporous structure of the 3D foam.[11, 12] However, this 3D sensor only exhibits selective detection of DA in the presence of UA, attributed to the weak specific interaction of the single electrode material (graphene) with DA. Another shortcoming is that the 3D material needs to be fixed on a supporting substrate to give a final electrochemical electrode, which decreases its flexibility and complicates its fabrication process. Chitosan (CHI) was reported to be a suitable support material with high mechanical strength to stabilize graphene in an electrochemical sensing electrode and provide a favorable interface for graphene-DA interaction.[9, 13] Vacuum stripped graphene (VSG) is composed of interconnected graphene nanoflakes, giving a 3D mesoporous microstructure which significantly increases the active surface area for reactions with small molecules.[14] Polypyrole (PPy) is an excellent conducting polymer with high stability and good biocompatibility, and hence is suitable for biosensing application.[6, 7] The motivation of the current work is therefore to design and tailor a 3D porous electrode using the above materials, so as to realize an electrode with high active surface area, high conductivity and strong selective interactions with DA, and high flexibility and free-standing ability, to achieve high performance DA sensor with enhanced sensitivity and selectivity.

In this work, we present a new type of hierarchical porous chitosan/vacuum-stripped graphene/polypyrrole (CHI/VSG/PPy) scaffold as a free-standing and flexible DA electrochemical sensor. The three scaffold materials were selected due to their specific interactions with DA and favorable physical properties,[6, 7, 9, 13] and the hierarchical porous scaffold structure was designed to provide high active surface area.[15] The CHI/VSG/PPy scaffold was prepared via a two-step process. As the electrode substrate, CHI/VSG scaffold was first fabricated using an ice segregation induced self-assembly (ISISA) technique which is a versatile and green bottom-up approach to produce aligned macroporous or layered materials.[14] Briefly, graphite oxide was first prepared via modified hummers' method[16, 17] and was then heated at 250 °C for 5 min under vacuum condition to obtain VSG. Homogenous CHI/VSG suspension in a syringe was unidirectionally dipped into liquid nitrogen at a constant dipping rate and then freeze-dried, giving rise to self-supported sponge-like 3D CHI/VSG scaffold with hierarchical porous structure composed of macropores formed by layered-branched architecture and meso/micropores from porous VSG uniformly covered and

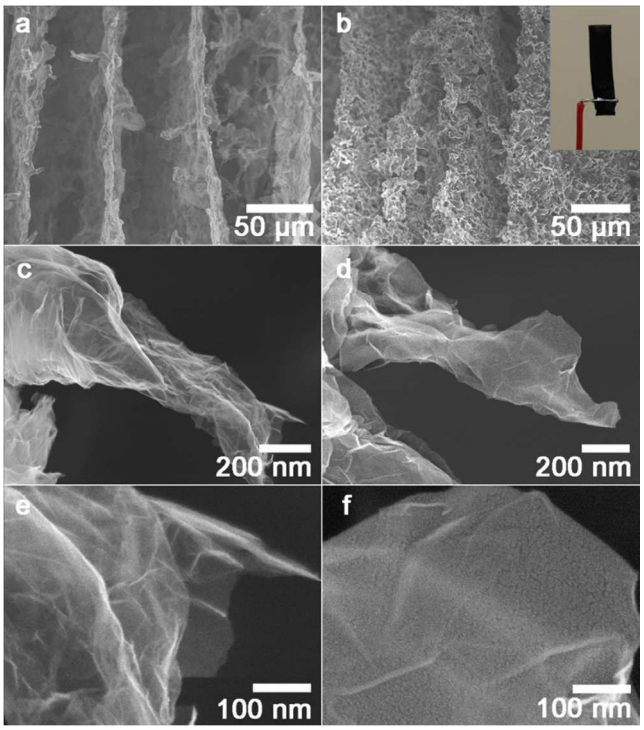

Fig. 1 FESEM images of CHI/VSG scaffold (a,c,e) and CHI/VSG/PPy scaffold (b,d,f) at different magnifications. Inset: A photograph of the 3D free-standing electrode.

embedded on the macroporous chitosan backbones (Fig. 1a and Fig.S2a). For comparison, pure CHI scaffold was also prepared, and the FESEM image and photograph are shown in Fig. S2b. The 3D CHI/VSG scaffold shows large specific surface area of 258.3 m^2 g^{-1} (Fig. S3), high flexibility and good elastic property, which favours high sensitivity, good stability and easy transportability, making it an ideal sensor substrate.[14] Subsequently, PPy was grown on the scaffold using an electropolymerization method (see ESI† for experimental details). The scaffold maintains its 3D sponge-like morphology (inset of Fig. 1b) after PPy loading, with well-aligned layered structure of 30-50 μm layer spacing (Fig. 1b), good flexibility and elastic properties, while its specific surface area slightly decreases to 226.0 m^2 g^{-1} compared to the original CHI/VSG scaffold as shown in Fig. S3. The porous VSG is composed of interconnected graphene flakes (Fig. S2a) which fully covers the layered-branched architecture of the scaffolds, forming continuous conduction network which should facilitate fast charge transfer. After incorporation of PPy into the CHI/VSG scaffold, VSG maintains its original porous structure as observed in Fig. 1c and 1d, making the internal surface of VSG available for reaction with DA. From the comparison of high-magnification FESEM images in Fig. 1e and 1f, nanostructured PPy on graphene flakes can be clearly identified for CHI/VSG/PPy scaffold, compared to the graphene flakes of the CHI/VSG scaffold, indicating the successful deposition of PPy on the scaffold. With the good flexible and elastic properties, the CHI/VSG/PPy scaffold can be directly connected with an electrical lead using epoxy as sealant for preparation of free-standing sensing electrode as shown in the inset of Fig. 1b.

Fig. 2a shows the Fourier transform infrared (FTIR) spectra of pure PPy, CHI/VSG and CHI/VSG/PPy scaffolds. The spectrum

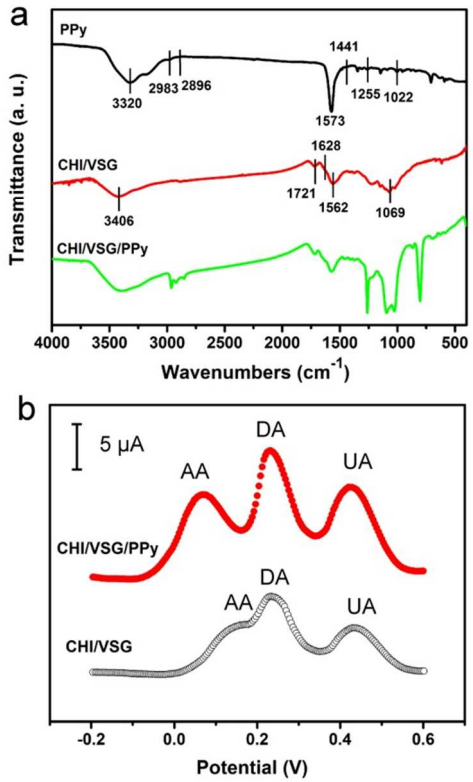

Fig. 2 (a) FTIR spectra of CHI/VSG and CHI/VSG/PPy scaffold. (b) DPV of 40 μM DA in the presence of 0.2 mM AA and 0.2 mM UA recorded at CHI/VSG electrode and CHI/VSG/PPy electrode in 0.1 M PBS (pH=6.0). Scan rate: 50 mV/s, pulse width: 200 ms.

of PPy exhibits peaks at 3320 cm^{-1}, 1573 cm^{-1} and 1441 cm^{-1}, corresponding to the N–H, C–C and C–N stretching vibrations in the pyrrole ring, respectively. The peaks at 2983 cm^{-1} and 2896 cm^{-1} are associated with the asymmetric stretching and symmetric vibration of CH_2. The peaks centered at 1255 cm^{-1} and 1022 cm^{-1} are designated to the C–N stretching and C–H deformation vibrations of PPy.[6, 18] The peaks at 3406 cm^{-1} and 1721 cm^{-1} in the spectrum of CHI/VSG are assigned to O–H, C–O stretching vibrations, respectively. C–O stretching along with N–H deformation mode and the stretching vibration mode of the hydroxyl group of chitosan are reflected in the peaks at 1628 cm^{-1} and 1069 cm^{-1}, respectively.[19] The peak at 1562 cm^{-1} can be attributed to the C–C skeleton vibration of the carbon rings in graphene.[18] All these characteristic peaks observed from the FTIR spectrum of CHI/VSG/PPy evidence the successful electrochemical polymerization of PPy on CHI/VSG scaffold. We speculate that the peak at 800 cm^{-1} may be due to the presence of additional bonds formed between the pyrrole radical cations and residual carboxyl groups of VSG during the electrochemical polymerization step.

To investigate the effects of the scaffold materials on the selectivity of the sensor for DA detection, differential pulse voltammetry (DPV) measurements were carried out on CHI/VSG and CHI/VSG/PPy electrodes in 0.1 M phosphate buffer solution (PBS) containing 40 μM DA, 0.2 mM AA and 0.2 mM UA. The results in Fig. 2b show that both CHI/VSG and CHI/VSG/PPy electrodes could electrochemically distinguish the voltammetric peaks of DA and UA, which is could be attributed to the strong π-π interaction between graphene basal plane and phenyl ring of

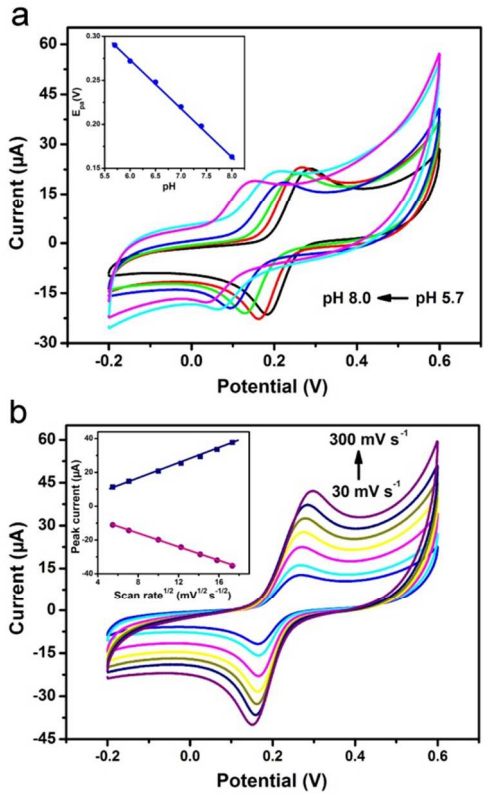

Fig. 3 (a) CVs of 40 μM DA at the CHI/VSG/PPy electrode in 0.1 M PBS at different pH. Inset: the linear relationship between the peak potential and pH. (b) CVs of 40 μM DA at the CHI/VSG/PPy electrode at different scan rates in 0.1 M PBS (pH=6.0). Inset: the relationship between the peak current and the square root of scan rate.

DA molecules,[11] leading to enhanced and specific voltammetric response of DA, and the separation of voltammetric peaks for DA-UA. The separation of DPV peak potentials for AA-DA was determined to be 0.098 V on CHI/VSG and 0.164 V on CHI/VSG/PPy. Although the CHI/VSG electrode shows overlapped voltammetric peaks for AA-DA, the peak separation of AA-DA on CHI/VSG (0.098 V) is still larger than that on a graphene modified GCE (~0.05V),[6] which may be due to the beneficial effects of the surface charges of the incorporated CHI[9, 13] For CHI/VSG/PPy electrode, the three distinct voltammetric peaks for AA, DA and UA could be observed, with peak potential at 0.068, 0.232, and 0.42 V, respectively. The wide separation of DPV peak potentials for AA-DA on CHI/VSG/PPy electrode is attributed to the electrodeposited PPy, which provides a selective interface due to its amine groups (–NH–) for molecular interaction with AA and has a strong electrocatalytic activity towards the oxidation of the three species,[6, 20, 21] resolving the overlapped voltammetric response of AA-DA and substantially, increasing the DPV peak currents for AA, DA and UA.

To determine the optimal pH for DA sensing performance evaluation, the effect of pH of the buffer solution on the electrochemical behaviour of DA was investigated by varying the pH of the 0.1 M PBS for cyclic voltammetry (CV) measurements. As shown in Fig. 3a, a pair of well-defined redox peaks is observed at the CHI/VSG/PPy electrode with the pH from 5.7 to 8.0. Both anodic and cathodic peak potentials (E_{pa} and E_{pc}) shift negatively with increasing pH, indicating the existence of proton transfer at the CHI/VSG/PPy electrode in the redox reaction of

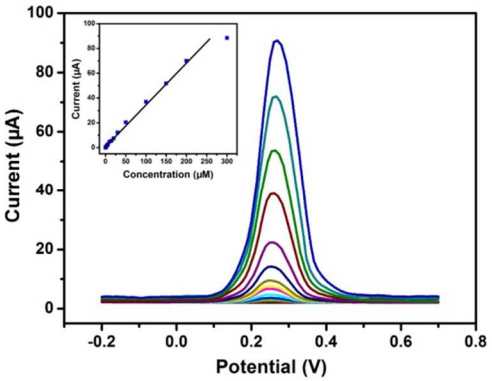

Fig. 4 DPVs of CHI/VSG/PPy electrode in 0.1 M PBS (pH=6.0) containing various concentrations of DA. From bottom to top DA concentration= 0, 0.1, 0.4, 1, 2, 4, 6, 10, 15, 20, 30, 50, 100, 150, 200, 300 μM. Inset: the relation between the peak current and the DA concentration.

DA.[22] A linear relationship is observed for the plot of E_{pa} *versus* pH (inset of Fig.3a), with a slope of −55 mV pH^{-1} which is very close to the theoretical value of −59 mV pH^{-1}, indicating that equal numbers of electrons and protons are involved in the electrochemical reaction of DA at CHI/VSG/PPy electrode.[22] The separation between E_{pa} and E_{pc} (ΔE_p) at different pH falls in the range of 0.103~0.123 V, with minimum ΔE_p at pH of 6.0. Moreover, the ratio of anodic to cathodic peak current (i_{pa}/i_{pc}) varies with pH, with minimum value of 1.04 at pH of 6.0, demonstrating a quasireversible redox reaction and a favourable electron transfer process for DA. As maximum peak current is observed at pH 6.0, PBS solution at this pH was selected for all the electrochemical characterizations of DA.

To study the effect of scan rate on the peak current of DA, CV measurements were carried out in 0.1 M PBS (pH 6.0) containing 40 μM DA by varying the scan rate and the results are shown in Fig. 3b. A linear relationship between peak current and square root of scan rate in the range of 50-300 mV s^{-1} is observed in the inset of Fig. 3b, illustrating that the reaction of DA at CHI/VSG/PPy electrode is a diffusion controlled process,[7, 23, 24]which may be attributed to the long diffusion pathway inside the scaffold for DA penetration due to the hierarchical porous structure of CHI/VSG/PPy scaffold.

To determine the calibration curve and DA detection limit of CHI/VSG/PPy electrode, DPV measurements were carried out. Fig. 4 shows the voltammetric responses of CHI/VSG/PPy electrode to the DA with various concentrations from 0.1 to 300 μM. As shown in the calibration curve (inset of Fig. 4), the plot of i_{pa} *versus* DA concentration shows good linearity in DA concentration range of 0.1-200 μM. The linear regression equation is calculated to be i_{pa} (μA)=0.6347+0.3493 C_{DA}(μM), with a correlation coefficient of 0.9981 and a detection limit of 19.4 nM (*S/N*=3). The sensitivity of the CHI/VSG/PPy scaffold sensor is normalized to the lateral area of the scaffold for easy comparison with other DA sensors and the normalized sensitivity is 632.1 μA mM^{-1} cm^{-2}. The determination of DA was also performed in the presence of 0.2 mM AA (ESI Fig. S4), and the linear regression equation was determined to be i_{pa} (μA)=0.8191+0.3506 C_{DA}(μM), with a correlation coefficient of 0.9976. The slope of the calibration curve obtained in the presence and absence of interfering species are almost the constant, which indicates that the sensor performance was not

influenced by the interfering molecules. The analytical performance of the CHI/VSG/PPy electrode outperforms previously reported graphene modified and/or PPy modified planar electrode and 3D graphene foam electrode, and exhibits comparable performance with Au modified electrode (Table 1). The high sensitivity, good selectivity and wide linear range are attributed to the large active surface area of the scaffold from its hierarchical porous structure for extensive reaction with DA, continuous VSG network for fast charge transfer, strong π-π interaction between graphene basal plane and phenyl ring of DA molecules for enhanced voltammetric response and discrimination of DA from UA, and the selective interface and functional groups of PPy and CHI for enhanced selective interaction with DA.

Table 1 Analytical characteristics for electrochemical detection of DA at different electrodes.

Electrode	Interferents	Linear range (μM)	Detection limit (nM)	Ref
PPyox/GR/GCE[a]	AA	0.5-10	100	7
PPy/rGO/GCE[b]	AA, UA	0.1-150	23	6
GR/GCE	AA	4-100	2.64	8
GR-CHI/GCE	AA, UA	5-200	–	9
3D GR foam	UA	~25	25	11
PPyox/MWCNT/GCE[c]	AA, UA	1-50	380	25
AuNPs@SiO2-MIPs[d]	AA, UA	0.048-50	20	26
CHI/VSG/PPy scaffold	AA, UA	0.1-200	19.4	This work

[a] PPyox: overoxidized polypyrrole. GR: graphene. [b] rGO: reduced graphene oxide. [c] MWCNT: multiwalled carbon nanotube. [d] NP: nanoparticle. MIP: molecularly imprinted polymer.

To evaluate the practicality of the CHI/VSG/PPy electrode in real biological samples, determination of DA in human serum was conducted. The concentrations of AA, UA and DA in human blood serum were reported to be 0.125 mM, 0.330 mM and 8.5-79 nM, respectively.[6, 27] The pre-determined concentrations of standard DA solution were spiked into the corresponding blood serum. The observed high recovery of 98-104 % with small relative standard deviations (RSD) (refer to ESI Table S1) of the CHI/VSG/PPy electrode indicates that the CHI/VSG/PPy electrode is a suitable sensing electrode for the determination of DA in real blood serum samples.

The reproducibility and stability of the CHI/VSG/PPy sensor were evaluated by a continuous DPV scanning of three identical electrodes prepared using same procedure with a time interval of three days (in 0.1 M PBS solution containing 40 μM DA) for two weeks. The RSD of sensitivity to DA is 3.73 %, confirming that the fabrication method was highly reproducible. A slight current drop of 2.67 % was observed during the first three days, and finally 90.08 % of the initial current response remained after two weeks (Fig. S5). The good repeatability and stability of the proposed sensor could be ascribed to the good stability of VSG and the strong interaction between PPy and graphene.

In summary, a metal-catalyst free three dimensional DA electrochemical sensor has been successfully developed based on a novel hierarchical porous CHI/VSG/PPy scaffold prepared via a two-step strategy containing freeze-casting and electrochemical polymerization techniques. Its hierarchical porous structure enlarges the available active surface area of the sensing electrode for the reaction with DA. CHI, utilized as the backbone of the electrode, provides flexible and elastic properties to the free-standing electrode and thus simplifying the electrode fabrication process. The synergistic interactions of the three scaffold components significantly increase the specific voltammetric response of DA and inhibit the interference of UA and AA. Overall, a careful material selection and good scaffold structure design contribute to the superior DA sensing performance of the CHI/VSG/PPy electrode.

Notes and references

[a] *School of Chemical and Biomedical Engineering, Nanyang Technological University, 62 Nanyang Drive, 637459 Singapore. Fax: 65-65921614; Tel: 65-63168829; E-mail: tytan@ntu.edu.sg*

† Electronic Supplementary Information (ESI) available: Detailed experimental procedures, FESEM image of VSG, BET results and photograph of the sensing electrode. See DOI: 10.1039/b000000x/

1. J. Weng, J. M. Xue, J. Wang, J. S. Ye, H. F. Cui, F. S. Sheu and Q. Q. Zhang, *Advanced Functional Materials*, 2005, **15**, 639-647.
2. B. Fabre and L. Taillebois, *Chemical Communications*, 2003, 2982-2983.
3. K. Jackowska and P. Krysinski, *Analytical and Bioanalytical Chemistry*, 2013, **405**, 3753-3771.
4. J. F. Ping, J. A. Wu and Y. B. Ying, *Electrochemistry Communications*, 2010, **12**, 1738-1741.
5. K. Reddaiah, M. M. Reddy, P. Raghu and T. M. Reddy, *Colloids and Surfaces B-Biointerfaces*, 2013, **106**, 145-150.
6. P. Si, H. L. Chen, P. Kannan and D. H. Kim, *Analyst*, 2011, **136**, 5134-5138.
7. Z. J. Zhuang, J. Y. Li, R. A. Xu and D. Xiao, *International Journal of Electrochemical Science*, 2011, **6**, 2149-2161.
8. Y. R. Kim, S. Bong, Y. J. Kang, Y. Yang, R. K. Mahajan, J. S. Kim and H. Kim, *Biosensors & Bioelectronics*, 2010, **25**, 2366-2369.
9. Y. Wang, Y. M. Li, L. H. Tang, J. Lu and J. H. Li, *Electrochemistry Communications*, 2009, **11**, 889-892.
10. L. Y. Jin, X. Gao, L. S. Wang, Q. Wu, Z. C. Chen and X. F. Lin, *Journal of Electroanalytical Chemistry*, 2013, **692**, 1-8.
11. X. C. Dong, X. W. Wang, L. H. Wang, H. Song, H. Zhang, W. Huang and P. Chen, *Acs Applied Materials & Interfaces*, 2012, **4**, 3129-3133.
12. M. Zhou, Y. Zhai and S. Dong, *Analytical Chemistry*, 2009, **81**, 5603-5613.
13. D. X. Han, T. T. Han, C. S. Shan, A. Ivaska and L. Niu, *Electroanalysis*, 2010, **22**, 2001-2008.
14. Z. He, J. Liu, Y. Qiao, C. M. Li and T. T. Y. Tan, *Nano Letters*, 2012, **12**, 4738-4741.
15. M. Zhou and S. Dong, *Accounts of Chemical Research*, 2011, **44**, 1232-1243.
16. Z. He, G. Guai, J. Liu, C. Guo, J. S. Chye Loo, C. M. Li and T. T. Y. Tan, *Nanoscale*, 2011, **3**, 4613-4616.
17. Z. He, H. Phan, J. Liu, T.-Q. Nguyen and T. T. Y. Tan, *Advanced Materials*, 2013, DOI: 10.1002/adma.201303327.

18. W. D. Lin, H. M. Chang and R. J. Wu, *Sensors and Actuators B-Chemical*, 2013, **181**, 326-331.
19. B. Batra and C. S. Pundir, *Biosensors & Bioelectronics*, 2013, **47**, 496-501.
20. Z. Q. Gao and H. Huang, *Chemical Communications*, 1998, 2107-2108.
21. S. Shahrokhian and H. R. Zare-Mehrjardi, *Electroanalysis*, 2009, **21**, 157-164.
22. Y. Y. Wu, L. L. Cui, Y. Liu, G. J. Lv, T. Pu, D. J. Liu and X. Q. He, *Analyst*, 2013, **138**, 1204-1211.
23. J. Liu, Y. Qiao, Z. S. Lu, H. Song and C. M. Li, *Electrochemistry Communications*, 2012, **15**, 50-53.
24. J. Liu, Y. Qiao, C. X. Guo, S. Lim, H. Song and C. M. Li, *Bioresour. Technol.*, 2012, **114**, 275-280.
25. Y. X. Li, P. Wang, L. Wang and X. Q. Lin, *Biosensors & Bioelectronics*, 2007, **22**, 3120-3125.
26. D. J. Yu, Y. B. Zeng, Y. X. Qi, T. S. Zhou and G. Y. Shi, *Biosensors & Bioelectronics*, 2012, **38**, 270-277.
27. B. Liu, H. T. Lian, J. F. Yin and X. Y. Sun, *Electrochimica Acta*, 2012, **75**, 108-114.